Microscale Enzymatic Optical Biosensors Using Mass Transport Limiting Nanofilms. 2. Response Modulation by Varying Analyte Transport Properties

ARTICLE *in* ANALYTICAL CHEMISTRY · APRIL 2008

Impact Factor: 5.64 · DOI: 10.1021/ac701738e · Source: PubMed

3 AUTHORS, INCLUDING:

Michael J McShane
Texas A&M University
180 PUBLICATIONS **3,309** CITATIONS

SEE PROFILE

Anal. Chem. **2008,** *80,* 1408−1417

Microscale Enzymatic Optical Biosensors Using Mass Transport Limiting Nanofilms. 2. Response Modulation by Varying Analyte Transport Properties

Erich W. Stein,[†,‡,§] Saurabh Singh,[∥] and Michael J. McShane*[,†,‡,∥]

Biomedical Engineering Program and Institute for Micromanufacturing, Louisiana Tech University, Ruston, Louisiana 71272, Department of Biomedical Engineering, Washington University in St. Louis, St. Louis, Missouri 63130, and Department of Biomedical Engineering, Texas A&M University, College Station, Texas 77843

Microscale implantable fluorescent sensors that can be transdermally interrogated using light are being pursued as a minimally invasive biochemical monitoring technology for in vivo applications. Previously, we reported the development of an enzymatic-based sensing platform characterized using glucose as a model biochemical analyte for minimally invasive diabetic monitoring. In this work, surface-adsorbed polyelectrolyte nanofilms were employed to modulate the relative fluxes of glucose and oxygen into the sensor, allowing response characteristics, namely, analytical range and sensitivity, to be tuned. Modulation of substrate transport properties were obtained by varying surface-adsorbed nanofilm thicknesses, ionic strength of assembly conditions, and outermost constituents. In general, increasing film thickness through additional cycles of adsorption resulted in consistently decreased glucose flux, correspondingly decreasing sensitivity and increasing range. While the two components of the nanofilms remained the same [poly(allylamine hydrochloride), PAH; poly(sodium 4-styrenesulfonate)}, the assembly conditions and terminal layer were found to strongly influence sensor behavior. Specifically, without added salt in assembly conditions, glucose diffusion was significantly decreased when films were capped with PAH, resulting in reduced sensitivity and extended range of response. With added salt, however, sensor response was the same for films of the same thickness but different terminal materials. These findings demonstrate that sensor response may be customized to cover the hypo- (0−80 mg/dL), normo- (80−120 mg/dL), and hyperglycemic levels (>120 mg/dL) from a single batch of particles through appropriate selection of coating structure and assembly conditions. Furthermore, the results indicate nanofilms of only 12-nm thickness could significantly affect response behavior, confirming predicted behavior by models of sensor reaction−diffusion kinetics. These findings demonstrate the ability to engineer sensor response properties using a simple, cost-effective means and lay the groundwork for developing additional highly sensitive biochemical monitors.

Real-time biochemical monitors would enable a unique means for clinicians and researchers to investigate and monitor the status of living systems. Moreover, the ability to provide sensitive, real-time measurements at the point of care could improve early-onset diagnosis and management of ailments arising from chemical imbalances.[1] Optical biosensors—particularly those based on fluorescence techniques—are attractive for such situations due to the high sensitivity and selectivity for desired analytes and the potential for minimally invasive analysis.[2−4] One concept for biochemical monitoring that could provide both continuous and spot measurements relies upon minimally invasive functional implants comprising a population of microscale particles; by design, with an appropriate optical transduction approach, these implants could be interrogated with light to obtain measurements for specific biochemical targets.[5−10] Alternatively, the same microparticles containing multiple reagents packaged together could result in new, improved, faster, or simpler in vitro assays.

Of central importance in the design of such systems is the development of the analyte-sensing chemistry, as well as a suitable container that allows free analyte transport with minimal reagent leaching. Previous reports on encapsulated sensing approaches have employed analyte-dependent changes in resonance energy

* To whom correspondence should be addressed. Phone: (979) 845-7941. Fax: (979) 845-4450. E-mail: mcshane@tamu.edu.
† Biomedical Engineering Program, Louisiana Tech University.
‡ Institute for Micromanufacturing, Louisiana Tech University.
§ Washington University in St. Louis.
∥ Texas A&M University.

(1) Kohli-Seth, R.; Oropello, J. M. *Crit. Care Clin.* **2000**, *16*, 557−578, vii−viii.
(2) Wolfbeis, O. S. *J. Mater. Chem.* **2005**, *15*, 2657−2669.
(3) Pickup, J. C.; Hussain, F.; Evans, N. D.; Rolinski, O. J.; Birch, D. J. S. *Biosens. Bioelectron.* **2005**, *20*, 2555.
(4) Asian, K.; Lakowicz, J. R.; Geddes, C. D. *Anal. Chem.* **2005**, *77*, 2007.
(5) Stein, E. W.; Grant, P. S.; Zhu, H.; McShane, M. J. *Anal. Chem.* **2007**, *79*, 1339−1348.
(6) McShane, M. J. In *Topics in Fluorescence Spectroscopy*; Geddes, C. D., Lakowicz, J. R., Eds.; Springer: New York, 2006; Vol. 11.
(7) Ibey, B. L.; Pishko, M.; Cote, G. L. In *Topics in Fluorescence Spectroscopy*; Geddes, C. D., Lakowicz, J. R., Eds.; Springer: New York, 2006; Vol. 11.
(8) Brown, J. Q.; McShane, M. J. *Biosens. Bioelectron.* **2006**, *21*, 1760−1769.
(9) Chinnayelka, S.; McShane, M. J. *Anal. Chem.* **2005**, *77*, 5501−5511.
(10) Russell, R. J.; Pishko, M. V.; Gefrides, C. C.; McShane, M. J.; Cote, G. L. *Anal. Chem.* **1999**, *71*, 3126−3312.

10.1021/ac701738e CCC: $40.75
Published on Web 02/01/2008

transfer that occur during competitive binding (CB) between the target analyte and a fluorescent analogue, where the decoupling of a fluorescent ligand−receptor pair by the analyte causes measurable changes in emission spectra.[9−12] The sensitivity and stability of CB systems have been improved through the use of hollow polymeric microscale capsules[9] and microporated hydrogel spheres,[13] which minimize assay leakage while allowing movement of assay components.

Other successes have been reported using analyte-specific enzymatic reactions to indirectly monitor changes in analyte concentrations.[5,14] Optical enzymatic assays employ analyte-specific enzymes along with a fluorophore sensitive to a cosubstrate or product to indirectly monitor analyte concentrations. One example of a well-characterized assay relies on glucose oxidase (GOx), an enzyme that consumes glucose and oxygen and produces gluconic acid and hydrogen peroxide, to sense glucose levels. A number of reports have demonstrated successful detection of glucose using fluorophores sensitive to oxygen,[5,14,15] hydrogen peroxide,[16,17] and pH.[18]

Given the commercial availability of oxygen-sensitive fluorophores, as well as oxidases, early prototypes of enzymatic microspheres have primarily relied on oxygen-quenched luminescent dyes for optical transduction,[2,5,19,20] While the concept of oxidase-based sensing may seem trivial given the wealth of prior art in electrochemical[21] and optical sensing using fiber-optic probes,[2,22] an intricate balance of reaction−diffusion kinetics must be met to realize useful microscale devices.[8] As the analyte diffuses into the sensor and oxygen is consumed, oxygen replenishment must exceed that of the analyte, resulting in analyte-limited oxygen consumption and changes in spectral properties correlated with analyte levels.[6,14] Thus, it is critical to control relative substrate diffusivities into the catalytic region of the sensor to obtain analyte-sensitive measurements.

To control substrate diffusivities, it is commonplace to incorporate transport-limiting materials such as polyurethane and silicone in the design of enzymatic sensors.[8,23] One of the simplest methods involves the deposition of films composed of synthetic or naturally occurring polymer materials to entrap sensor components and limit substrate delivery.[24−29] Most of this work, however, has focused on developing relatively bulky fiber-optic and electrochemical biosensors, and the surface modification techniques proven successful (e.g., dip-coating) are procedurally difficult or impossible to obtain highly controllable, precise deposition required to modify the surface of microscale structures. Others have shown the sensor immobilization matrix can sufficiently control substrate diffusivities,[15,30] but fine-tuning sensor response properties with these techniques, while retaining enzyme reactivity would be procedurally difficult as well. Thus, a simple technique capable of depositing highly controlled, transport-limiting films on microstructures is desired as a means to precisely control substrate transport into enzyme-loaded microparticles to obtain analyte-sensitive measurements. Self-assembled multilayer nanofilms are one potential solution to this problem, and they offer an attractive means to study the effects of nanoscale films on sensor response.

Polyelectrolyte nanofilms fabricated using layer-by-layer self-assembly allow the construction of complex nanocomposite films through adsorption of oppositely charged molecules in a sequential fashion.[31,32] It has been demonstrated that certain polyelectrolyte nanofilms selectively inhibit transport of small molecules such as glucose, making this technique promising for use in creating nanoscale transport barriers for enzymatic-based biosensors.[33−38] Altering film assembly conditions, such as pH and ionic strength, and cross-linking between multilayers has been shown to alter thickness and permeability of polyelectrolyte nanofilms, suggesting additional means of tuning film permeabilities.[39,40] Furthermore, the outermost (capping) nanofilm layer has also been reported to have a profound effect on film permeability.[33] The current state of knowledge indicates that molecular transport through polyelectrolyte nanofilms is a highly complex phenomenon governed by nanofilm pore size, charge distribution, and hydrophobicity.[33,36,39,41,42] However, because this facile fabrication approach provides a means to alter film permeability with high precision, polyelectrolyte nanofilms are a model system to control substrate delivery in microscale enzymatic-based sensing systems.

In our previous studies, we employed the transport-limiting properties of polyelectrolyte nanofilms to design several generations of glucose-sensitive microspheres toward the goal of minimally invasive diabetic monitoring.[5,6,14] Most recently, we used microspheres prepared with a novel alginic acid−silicate matrix termed "algilica" to coimmobilize the key sensor ingredients GOx and Pt(II) porphyrins within the interior of the particles, while

(11) D'Auria, S.; DiCesare, N.; Staiano, M.; Gryczynski, Z.; Rossi, M.; Lakowicz, J. R. *Anal. Biochem.* **2002**, *303*, 138−144.
(12) Ge, X.; Tolosa, L.; Rao, G. *Anal. Chem.* **2004**, *76*, 1403.
(13) Rounds, R. M.; Ibey, B. L.; Beier, H. T.; Pishko, M. V.; Cote, G. L. *J. Fluoresc.* **2007**, *17*, 57−63.
(14) Brown, J. Q.; Srivastava, R.; McShane, M. J. *Biosens. Bioelectron.* **2005**, *21*, 212−216.
(15) Xu, H.; Aylott, J. W.; Kopelman, R. *Analyst* **2002**, *127*, 1471−1477.
(16) Schaferling, M.; Wu, M.; Wolfbeis, O. S. *J Fluoresc* **2004**, *14*, 561−568.
(17) Wolfbeis, O. S.; Durkop, A.; Wu, M.; Lin, Z. *Angew. Chem., Int. Ed.* **2002**, *41*, 4495.
(18) Trettnak, W.; Leiner, M. J. P.; Wolfbeis, O. S. *Biosensors* **1989**, *4*, 15.
(19) Amao, Y. *Microchim. Acta* **2003**, *143*, 1−12.
(20) Koo, Y.-E. L.; Cao, Y.; Kopelman, R.; Koo, S. M.; Brasuel, M.; Philbert, M. A. *Anal. Chem.* **2004**, *76*, 2498−2505.
(21) Bakker, E.; Qin, Y. *Anal. Chem.* **2006**, *78*, 3965−3984.
(22) Wolfbeis, O. S. *Anal. Chem.* **2006**, *78*, 3859−3874.
(23) Gough, D. A.; Lucisano, J. Y.; Tse, P. H. S. *Anal. Chem.* **1985**, *57*, 2351−2357.
(24) Trettnak, W.; Wolfbeis, O. S. *Anal. Chim. Acta* **1989**, *221*, 195−203.
(25) Wolfbeis, O. S.; Oehme, I.; Papkovskaya, N.; Klimant, I. *Biosens. Bioelectron.* **2000**, *15*, 69−76.
(26) Rosenzweig, Z.; Kopelman, R. *Anal. Chem.* **1996**, *68*, 1408−1413.
(27) Choi, H. N.; Kim, M. A.; Lee, W.-Y. *Anal. Chim. Acta* **2005**, *537*, 179−187.
(28) Wang, B.; Li, B.; Deng, Q.; Dong, S. *Anal. Chem.* **1998**, *70*, 3170−3174.
(29) Pandey, P. C.; Upadhyay, S.; Pathak, H. C. *Sens. Actuators, B: Chem.* **1999**, *B60*, 83−89.
(30) Wu, X. J.; Choi, M. M. F. *Anal. Chim. Acta* **2004**, *514*, 219−226.
(31) Schonhoff, M. *Curr. Opin. Colloid Interface Sci.* **2003**, *8*, 86−95.
(32) Lvov, Y. *Electrostatic layer-by-layer assembly of proteins and polyions*; M. Dekker: New York, 2000.
(33) Liu, X.; Bruening, M. L. *Chem. Mater.* **2004**, *16*, 351−357.
(34) Bruening, M. L.; Sullivan, D. M. *Chem.: Eur. J.* **2002**, *8*, 3832−3837.
(35) Miller, M. D.; Bruening, M. L. *Langmuir* **2004**, *20*, 11545−11551.
(36) Stanton, B. W.; Harris, J. J.; Miller, M. D.; Bruening, M. L. *Langmuir* **2003**, *19*, 7038−7042.
(37) Harris, J. J.; Stair, J. L.; Bruening, M. L. *Chem. Mater.* **2000**, *12*, 1941−1946.
(38) Miller, M. D.; Bruening, M. L. *Chem. Mater.* **2005**, *17*, 5375−5381.
(39) Dubas, S. T.; Schlenoff, J. B. *Macromolecules* **1999**, *32*, 8153−8160.
(40) Zhu, H. G.; McShane, M. J. *Langmuir* **2005**, *21*, 424−430.
(41) Steitz, R.; Leiner, V.; Siebrecht, R.; Klitzing, R. v. *Colloids Surf. A* **2000**, *163*, 63−70.
(42) Klitzing, R. v.; Möhwald, H. *Macromolecules* **1996**, *29*, 6901−6906.

surface-adsorbed polyelectrolyte nanofilms were deposited to control substrate diffusion.[5] When compared to our first-generation prototypes based on ruthenium complexes and hydrogel microspheres,[14] we observed an increase in glucose sensitivity (percent change of relative fluorescence intensities per mg/dL glucose) of ~100 times, due in large part to elevated oxygen sensitivity associated with the use of Pt(II) porphyrin complexes and the sol−gel matrix. While these results are promising, the analytical range of these devices was determined to be 2−120 mg/dL, significantly below the accepted clinical range of 40−350 mg/dL required for in vivo monitoring;[5] thus, an extension of the response range was desired.

Working toward the goal of developing clinically relevant glucose sensors, in this work, we aim to extend the analytical range of our sensor prototypes by modulating substrate transport into the sensor with variations in surface-adsorbed nanofilm thickness, ionic strength of assembly conditions, and capping layer. Since oxygen transport through polyelectrolyte nanofilms is less affected by nanofilm thickness than glucose (mainly due to size),[33] it is hypothesized that increasing nanofilm thickness would slow glucose transport (relative to oxygen) into the sensor, increasing the steady-state local oxygen levels and extending range. While this work uses glucose as a model analyte, this generalized approach may be applied in the rapid prototyping of additional biosensors by selecting appropriate enzymes, indicators, and diffusion-limiting coatings. Thus, this "mix and match" approach to sensor design lays the foundation for the future development of minimally invasive biochemical sensors that may find widespread use in areas ranging from the clinic to the battlefield.

EXPERIMENTAL DETAILS

Materials. Sodium alginate (low viscosity, 250 counts/s, MW 12−80 kDa), (3-glycidyloxypropyl)trimethoxysilane (GPTS), and ammonium hydroxide were obtained from Sigma and used for the synthesis of mesoporous alginate−silica particles. PtOEP (Frontier Scientific), tetrahydrofuran (THF, Fluka), GOx (type VII from *Aspergillus niger*, 198k units/g of solid, Sigma), *N*-(3-dimethylaminopropyl)-*N*′-ethylcarbodiimide hydrochloride (EDC, Fluka), *N*-hydroxysulfosuccinimide sodium salt (NHSS, Toronto Research Chemicals Inc.), and sodium acetate (Sigma) were used to prepare PtOEP/GOx-doped alginate−silica particles. Poly(allylamine hydrochloride) (PAH, MW 70 kDa, Aldrich), poly(sodium 4-styrenesulfonate) (PSS, MW 70 kDa, Aldrich), and sodium chloride (Sigma) were used during the deposition of multilayer thin films. Additionally, rhodamine B isothiocyanate (RITC, Aldrich) was conjugated to PAH and used in thin-film deposition. β-D-Glucose (MP Biomedicals, Inc.), O_2 and N_2 gas (Air Liquide), and phosphate-buffered saline (PBS, Sigma) were used during dynamic testing. All necessary pH adjustments were performed using titrations of 1.0 M HCl and 1.0 M NaOH (Fluka). All chemicals listed above were reagent grade and used as received. Throughout all experimental procedures, ultrapure water with a resistivity of greater than 18 MΩ was used. Unless otherwise stated, all experimental processes were conducted at 25 °C.

Preparation of Mesoporous Alginate−Silica Particles. Alginate−silica ("algilica") particles were prepared using a procedure similar to that described in our previous report.[5] Briefly, the precursor was prepared by stirring a solution composed of 1.5 wt % aqueous alginate solution and GPTS in a 1:1 volumetric ratio for at least 4 h, resulting in an alginate-modified silanol. While stirring, 2 mL of the precursor silanol was added to 3 mL of water. To initiate the sol−gel process, 1.25 mL of 10 M NH_4OH was added and the resultant mixture stirred for 20 min, followed by the addition of 10 mL of water and an additional stirring time of 40 min. An extra 40 mL of water was added and the suspension stirred for at least an additional 4 h. The resulting particle suspension was rinsed with DI water using four sequential centrifugation cycles and diluted to a total aqueous suspension volume of 1.5 mL. A Beckman Coulter counter (Z2) equipped with a 100-μm aperture was used to obtain the mean diameter and concentration of particles comprising the stock suspension.

Preparation of PtOEP and GOx-Doped Particles. Approximately 250 μL of stock particle suspension was placed in a microcentrifuge tube and dried under streaming N_2, followed by adding 250 μL of a 500 μM PtOEP solution prepared in THF. The container was sealed to prevent volatilization of THF and stirred for 30 min, after which 30 μL of water was added and the suspension stirred for an additional 30 min. The water added to the suspension initiated a solvent-mediated controlled precipitation of PtOEP into the mesoporous particles, a technique used in previous reports to aid in the immobilization of desired molecules.[43] The suspension was subsequently rinsed with DI water four times. Following the last rinse cycle, the supernatant was removed and 300 μL of 35 mg/mL GOx prepared in 0.05 M pH 4 sodium acetate buffer was added. The pH value was selected based on experimental results from our previous work.[5] The suspension was stirred for 1.5 h, followed by two rinsing cycles with DI water. The supernatant was subsequently removed and replaced with 250 μL of solution composed of 30 and 10 mg/mL EDC and NHSS in 0.05 M sodium acetate (pH 5.0) to catalyze amide bond formation between amine and carboxylic acid functionalities on GOx and alginate, respectively.[44] Finally, the suspension of PtOEP/GOx-doped particles was stirred for 4 h and then rinsed two times with DI water.

Adsorption of Nanofilm Surface Coatings. RITC was conjugated to PAH (PAH−RITC) according to a standard amine conjugation protocol.[45] Prior to multilayer film deposition, solutions of PSS, PAH, and PAH−RITC were prepared in 0.2 M NaCl at a concentration of 2 mg/mL. The supernatant of the PtOEP/GOx-doped particles was removed, and the particles were resuspended in PAH−RITC. Following a 15-min adsorption period, during which the particles were continuously vortexed, and protected from light with aluminum foil, the particles were rinsed three times with DI water and subsequently resuspended in PSS solution. It was previously determined that three bilayers of PAH−RITC and PSS (denoted $\{PAH-RITC/PSS\}_3$), was required to obtain a PtOEP emission maximum (645 nm) that was ~75% of the RITC emission maximum (585 nm); thus, all coated sensors received a base film of $\{PAH-RITC/PSS\}_3$. To investigate the effect of nanofilm thickness on response properties, uncoated sensors and sensors coated with 3, 5, 10, 15, 20, and 25 PAH/PSS bilayers were prepared and resuspended, such that particle concentrations

(43) Sukhorukov, G. L. D. J. H. E. D. H. M. *Adv. Mater.* **2000**, *12*, 112−115.
(44) Zhu, H.; Srivastava, R.; Brown, J. Q.; McShane, M. J. *Bioconjugate Chem.* **2005**, *16*, 1451−1458.
(45) Brinkley, M. *Bioconjugate Chem.* **1992**, *3*, 2−13.

across all samples were equivalent. To study the effect of assembly solution ionic strength and capping layer on sensor performance, additional sensors were prepared with 5, 10, and 15 PSS- or PAH-capped nanofilms assembled with solutions without added NaCl.

Dynamic Testing Apparatus. A custom dynamic testing apparatus and associate virtual instrument software control program (LabVIEW, National Instruments) was developed to monitor real-time changes in sensor response. The system allows control of bulk oxygen concentration by means of regulated mixing of oxygen and nitrogen through a pair of individually addressable pressure controllers (model 00122QA, Cole-Parmer Instrument Co.) for the buffer and glucose reservoirs, respectively. Equilibration of oxygen levels within each reservoir was hastened with gas diffusers (ChemGlass, fine frit) and magnetic assisted stirring (Dylastir, VWR). Desired glucose concentrations in the reaction chamber were obtained through mixing of glucose and buffer stock solutions extracted from the reservoirs by peristaltic pumps (MasterFlex L/S 7550 pump drive with MasterFlex Easy Load 3 pump heads). Prior to entering the reaction chamber, the bulk oxygen level of the glucose solution was recorded using an in-line oxygen microelectrode and picoammeter (OX 500 and PA2000, Unisense). The reaction chamber consists of a custom-designed Garolite (Cole Parmer) flow cell, which accepts a standard microscope slide (25 × 75 × 1 mm, VWR) with the sensors immobilized to the surface. Additionally, the reaction chamber contains a port to interface the sample slide with a custom optical fiber. The optical fiber probe was composed of one delivery fiber and six collection fibers (400 μm multimode, BFH37-400, Thor Labs), which was used to deliver excitation light from a Hg−Xe arc lamp (model 68811, Oriel) containing a 530 ± 5 nm interference filter (Thor Labs). Sensor emission was subsequently delivered to a CCD array spectrometer (USB 2000, OceanOptics) through the collection bundle. Following passage through the reaction chamber, outlet solution oxygen levels were recorded using an additional in-line microelectrode chamber prior to being collected as waste and discarded. It was determined that tubing in direct contact with solution (Norprene, MasterFlex) exhibited negligible oxygen permeability, thereby minimizing changes in oxygen levels as the solution traveled through the apparatus. A schematic of the testing system can be found in the first installment of this work.[5]

Due to relocation of the laboratory and upgrades, some changes to the instrumentation for sensor monitoring were implemented before the experiments to investigate the influence of assembly solution ionic strength and capping layer were performed. The second-generation testing platform employs a custom-designed fiber bundle (CeramOptec; 78 delivery and 41 collection 200-μm multimode fibers, 0.22 NA, silica clad), a 518-nm LED light source (Ocean Optics) passed through a 540 ± 10 nm filter, and a CCD array spectrometer (Ocean Optics; USB 4000, with grating matched to 500-800-nm spectral range).

Dynamic Glucose Sensitivity Testing. Large-volume reservoirs (4 L) supplied the testing apparatus with buffer and glucose, respectively. The buffer reservoir contained 0.01 M PBS (pH 7.4), while the glucose reservoir contained 600 mg/dL β-D-glucose dissolved in 0.01 M PBS (pH 7.4). It is noteworthy that the ionic strength of both reservoir solutions was kept constant throughout all experimental procedures. The oxygen levels in both reservoirs were equilibrated to air-saturated conditions. Sample preparation was performed as described above. Random triplicate glucose levels, ranging from 25 to 300 mg/dL in 25 mg/dL increments, were flowed through the reaction chamber at a rate of 4 mL/min for ~8 min at each concentration, parameters that were experimentally predetermined to minimize convective glucose transport while maintaining bulk oxygen levels. After initial glucose sensitivity experiments were performed under air-equilibrated conditions, sensor response to glucose at varying bulk oxygen was characterized at oxygen levels above and below air saturation, respectively. Spectral data were collected in real time throughout the course of the experiments. Later experiments used smaller increments of glucose concentration, as needed, to increase resolution of response profiles for highly sensitive particles and also employed increased duration of exposure at each concentration to ensure stabilization of the ratiometric response in each case.

Sensor Response Simulation. A mathematical model simulating the behavior of optical microscale enzymatic sensors was used to predict sensor response properties with varying thickness of adsorbed nanofilm as well as ambient oxygen levels, as detailed in a previous report.[8] Briefly, the modeling work involved solving the coupled system of differential equations describing the reaction−diffusion kinetics within a spherical geometry (*1*) to estimate the spatiotemporal sensor response to step changes in external glucose levels.

$$\frac{\partial C_G}{\partial t} = \frac{D_G}{r^2}\frac{\partial}{\partial r}\left(r^2\frac{\partial C_G}{\partial r}\right) - R_G(C_G, C_O, E_T)$$

$$\frac{\partial C_O}{\partial t} = \frac{D_O}{r^2}\frac{\partial}{\partial r}\left(r^2\frac{\partial C_O}{\partial r}\right) - R_O(C_G, C_O, E_T) \quad (1)$$

In these expressions, the concentrations of oxygen and glucose are given by C_O and C_G, E_T represents the total immobilized GOx concentration, R_O and R_G are the oxygen and glucose reaction terms, and r is the sensor radius. The schematic in Figure 1 depicts the sensor geometry used in the model, indicating enzyme and indicator dye location within the sensor matrix and polyelectrolyte nanofilms adsorbed to the matrix surface. Initial and boundary conditions as well as input parameters used for the model were experimentally determined or obtained from previous reports.[5,8,33,46−49] Average steady-state oxygen values within the sensors were calculated for a range of bulk glucose levels, and using calibration data previously reported,[5] average steady-state oxygen levels were converted into PtOEP/RITC peak ratios. Subsequently, these data were used to construct steady-state glucose response profiles similar to that shown in Figure 2 and the corresponding normalized sensitivities compared to experimental data.

RESULTS AND DISCUSSION

Dynamic and Steady-State Glucose Response. Sensor response was characterized with a custom flow chamber that

(46) Tse, P. H. S.; Gough, D. A. *Biotechnol. Bioeng.* **1987**, *29*, 705−713.
(47) Netrabukkana, R.; Lourvanij, K.; Rorrer, G. L. *Ind. Eng. Chem. Res.* **1996**, *35*, 458−464.
(48) McDonagh, C.; MacCraith, B. D.; McEvoy, A. K. *Anal. Chem.* **1998**, *70*, 45−50.
(49) Malikkides, C. O.; Weiland, R. H. *Biotechnol. Bioeng.* **1982**, *24*, 2419−2439.

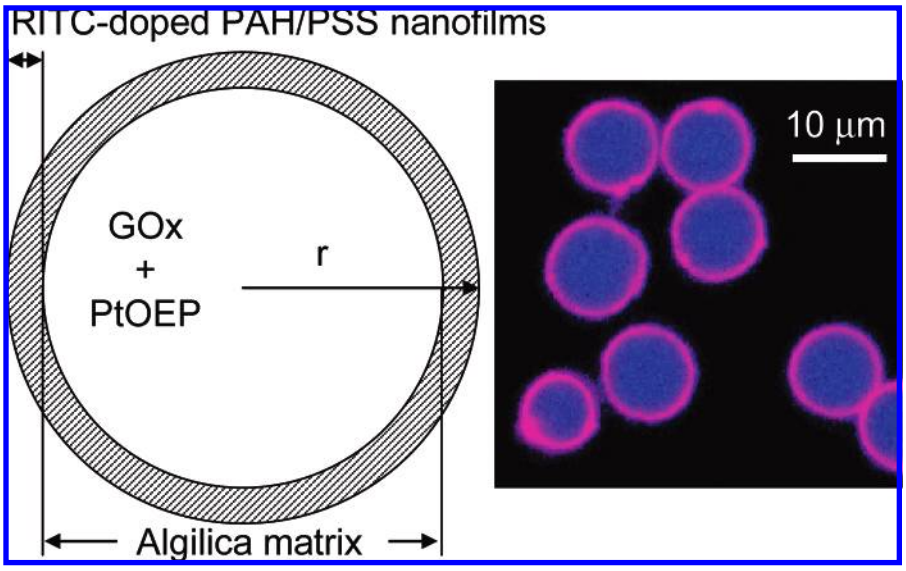

Figure 1. Schematic of enzymatic microparticle sensor and accompanying confocal micrograph depicting indicator (PtOEP, blue) and reference (RITC, pink) dye location.

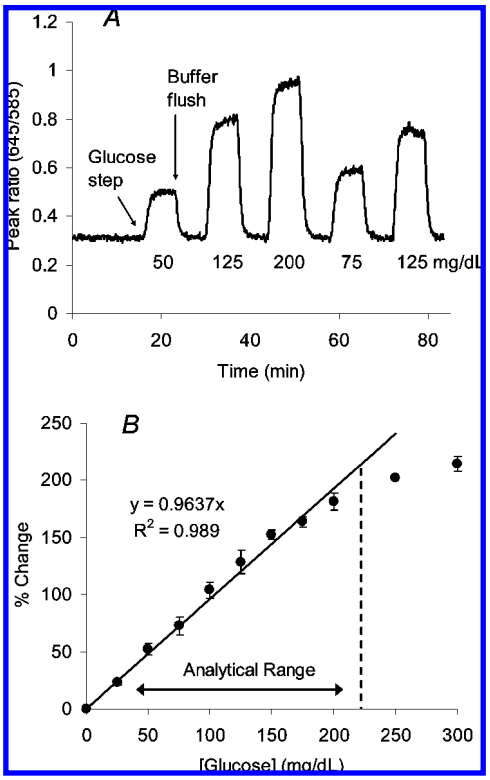

Figure 2. Typical sensor response to dynamic changes in bulk glucose levels (A) and resulting steady-state response profile (B) acquired from sensors with 25 surface-adsorbed PAH/PSS bilayers. Regression line is used to depict linear operation range, while analytical range (vertical line) indicates the point at which a 10% response deviation from linearity occurs. Error bars denote one standard deviation of random triplicate measurements.

dynamically controlled glucose and oxygen levels. In a typical experiment, sensors were exposed to step changes in bulk glucose levels followed by a buffer flush to remove glucose from the reaction chamber. The peak intensities of the indicator dye (PtOEP, 645 nm) and reference dye (RITC, 585 nm) were collected in real time and the PtOEP/RITC peak ratio plotted versus time. Figure 2A contains a representative plot of typical data collected in these experiments. These data depict a signal increase following sensor exposure to glucose (Figure 2A, marked "glucose step") resulting from the local depletion of oxygen levels arising from glucose oxidation. Furthermore, as glucose is removed from the reaction chamber (Figure 2A, marked "buffer flush"), the signal returns to baseline when remaining local glucose molecules are oxidized and local oxygen levels return to those of the bulk. In the first paper, we used similar dynamic data to characterize several figures of merit, including reversibility, stability, and response time.[5] While these characteristics are important, the sensitivity and analytical range are arguably the most critical when evaluating sensor feasibility for a given application. In order to determine the range and sensitivity of the devices, a steady-state response profile was generated by calculating the percent change of the PtOEP/RITC peak ratio (determined by average the 25 data points collected before buffer flushing) with respect to the baseline for each bulk glucose concentration (Figure 2B). Using these data, the sensitivity was obtained by calculating the slope of the linear region, defined as the range over which $R^2 \geq 0.95$. The analytical range was calculated by determining the lowest glucose concentration at which a 10% deviation from linearity is observed. In this work, we use "analytical range" as a synonym to "dynamic range", with one minor exception. In the first installment, we characterized the lower limit of the analytical range using the following relationship:

$$\mathrm{CQL} = 10\sigma_{\mathrm{baseline}}/S$$

where $\sigma_{\mathrm{baseline}}$ is baseline standard deviation and S is response sensitivity. Given the high sensitivity of these systems, the lower detection limit is smaller than our overall range by 2 orders of magnitude; thus, this calculation was not included in defining analytical range. Sensitivity and analytical range will be used in this work to evaluate sensor performance under several conditions, including the variations in surface-adsorbed nanofilm thickness, assembly conditions, and bulk oxygen level.

Effect of Nanofilm Thickness on Sensor Response. Successful realization of analyte-sensitive enzymatic smart tattoos

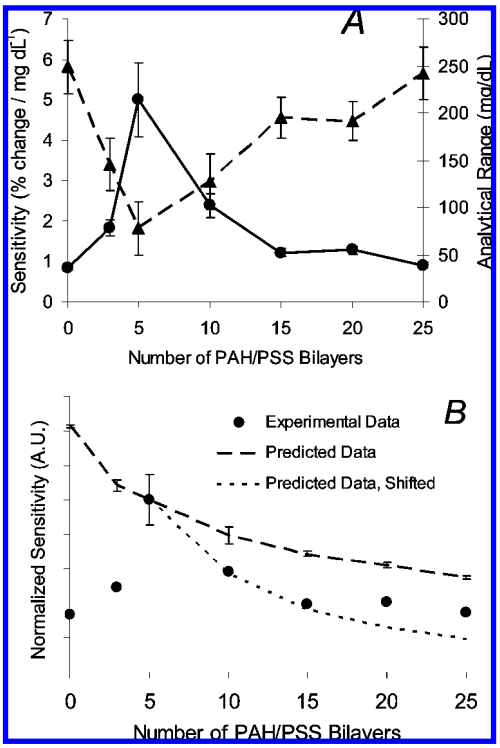

Figure 3. A() Effect of surface-adsorbed nanofilms on device sensitivity (●) and analytical range (▲) acquired under air-equilibrated oxygen conditions. Error bars donate one standard deviation of triplicate measurements. (B) Comparison of normalized predicted (—), predicted, and shifted (-), and experimentally obtained (●) sensitivity profiles of sensors with varying nanofilm bilayers.

relies on an intricate balance of substrate reaction-diffusion kinetics.[8,50] We employed surface-adsorbed polyelectrolyte nanofilms to precisely modulate glucose flux relative to that of oxygen (J_G/J_O) into the sensor, allowing sensor response characteristics to be tuned.

Sensors comprising various nanofilm thicknesses were subsequently tested and the analytical range and sensitivity for each case determined. These values were plotted against the respective number of PAH/PSS bilayers adsorbed to the sensor surface (Figure 3). Note that uncoated sensors contained no reference signal; thus, baseline drift was manually corrected following data acquisition. Interestingly, these data exhibit a local sensitivity maximum and accompanying range minimums at $\{PSS/PAH\}_5$; therefore, the discussion will begin by focusing on response characteristics observed with $\{PSS/PAH\}_{0-5}$-coated sensors and then continue to those of $\{PSS/PAH\}_{5-25}$-coated sensors.

It is important to note from the beginning that uncoated sensors (0 PAH/PSS bilayers) are indeed responsive to glucose. This observation is counter to previous experimental and theoretical explorations of sensors based on uncoated alginate hydrogel microparticles, which indicate rapid oxygen depletion and limited analytical range.[8] Thus, the response observed without transport-controlling coatings indicates that the algilica matrix used in this work presents a different relative permeability to glucose and oxygen than alginate. Indeed, it is well-known that similar silica-containing matrixes exhibit glucose diffusivities similar to those observed in water with greater oxygen diffusivities (~2 orders of magnitude) than hydrogel matrixes, indicating that the substrate itself significantly reduces J_G/J_O; the result is the observation of a glucose-sensitive response over extended ranges (hundreds of mg/dL) without transport-limiting coatings.[47,48] Further characterization of substrate transport through the algilica substrates used in this work is currently underway; however, the absolute substrate diffusivities through the matrix are not important to this study, which aims to establish the impact of the coatings on the sensor response properties.

Starting with uncoated particles, we observed an increase in device sensitivity with sequential increases in nanofilm bilayers, peaking at $\{PSS/PAH\}_5$. This is indeed unexpected, based on the comparison of theoretical and experimentally obtained data of device sensitivity with $\{PAH/PSS\}_{0-5}$ (Figure 3B). The mathematical models predict an exponential decrease in sensitivity with sensors comprising $\{PAH/PSS\}_{0-5}$ bilayers, a trend arising from incremental variations in relative substrate fluxes with sequential adsorption of nanofilm bilayers. However, the simulations assume each nanofilm bilayer is contiguous and homogeneous, an ideal situation reported to be inaccurate under experimental conditions.[51] On the basis of these previous findings, it is believed that initial coatings, i.e., $\{PSS/PAH\}_{3-5}$ are insufficient to achieve complete surface coverage of the sensor, resulting in a "leaky" diffusion barrier with a smaller effective thickness than expected. As a result, the reaction−diffusion kinetics are governed to a greater extent by substrate transport through the sphere matrix. However, the experimental data show behavior that is still influenced by the initial coatings rather than constant sensitivity; to further explain this behavior, the possibility that inhomogeneous nanofilm adsorption could indeed affect relative delivery rates of glucose and oxygen must be considered.

Previous reports have hypothesized that rapid oxygen diffusivities observed in silica-based matrixes are due to surface adsorption of dissolved oxygen, followed by rapid diffusion across the surface, while others report glucose diffusivities similar to water.[47,48,52] Thus, it is possible that the incomplete nanofilm surface coverage leaves substantial holes through which glucose may easily diffuse, minimally affecting glucose delivery into the sensor. In contrast, the adsorption of the polymers may hinder oxygen adsorption and subsequent transport across the surface of the substrate, ultimately resulting in an increased J_G/J_O and a correspondingly increased sensitivity. Experimental support for this theory was obtained by comparing the steady-state glucose response curves of sensors coated with $\{PSS/PAH\}_{0-5}$ (Figure 4). From these data, it is apparent that the maximum percent change and sensitivity are directly proportional to adsorbed nanofilm bilayers. Since PtOEP is readily quenched by molecular oxygen (i.e., emission intensity increases as oxygen levels decrease), increasing percent change values for each bilayer number at a given glucose level are a direct result of lower steady-state oxygen levels within the sensor. Furthermore, as a consequence of reduced local steady-state oxygen levels, sensors coated with $\{PSS/PAH\}_{0-5}$ become oxygen-limited at increasingly lower bulk glucose levels and subsequently higher sensitivities are observed. Decreased steady-state oxygen levels, coupled with increased sensitivity with respect to 0−5 nanofilm bilayers, indicate

(50) Leypoldt, J. K.; Gough, D. A. *Anal. Chem.* **1984**, *56*, 2896−2904.
(51) Ai, H.; Lvov, Y. M.; Mills, D. K.; Jennings, M.; Alexander, J. S.; Jones, S. A. *Cell Biochem. Biophys.* **2003**, *38*, 103−114.
(52) Han, B.-H.; Manners, I.; Winnik, M. A. *Chem. Mater.* **2005**, *17*, 3160−3171.

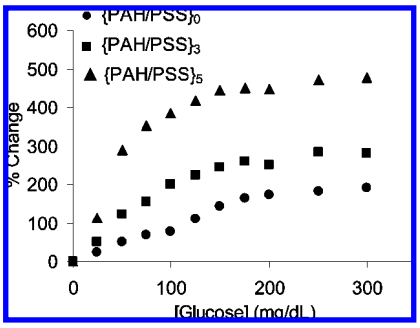

Figure 4. Steady-state glucose response profiles of sensors with 0 (●), 3 (■), and 5 (▲) PAH/PSS bilayers. Values represent means calculated from random triplicate measurements.

that J_G/J_O is sequentially increased with the application of {PSS/PAH}$_{0-5}$. This observation, combined with other reports that complete PAH/PSS nanofilms reduce J_G/J_O by 3 orders of magnitude,[33] suggests that {PSS/PAH}$_{3-5}$ coatings do not provide the complete surface coverage required to reduce glucose transport (relative to oxygen) but still significantly hinder oxygen transport (relative to glucose) across the substrate surface. This suggestion emphasizes that multilayer film deposition, although procedurally simple, is highly complex and governed by a multitude of environmental and physical properties, as shown by others.[53,54] Nonetheless, while this observation does give insight on the behavior of {PSS/PAH}$_{0-5}$ sensors, the key in a practical sense is that the adsorption of {PSS/PAH}$_5$ nanofilms results in a mean sensitivity increase of 0.3% /mg dL^{-1} (500% total) and range decrease of 34.3 mg/dL (70% total) per PAH/PSS bilayer and is therefore indeed an effective tool in modulating device sensitivity.

Following the initial increase in sensitivity between {PAH/PSS}$_{0-5}$-coated sensors, the theoretically predicted trend (exponential decrease in device sensitivity with increased nanofilm thickness) is observed with {PAH/PSS}$_{5-25}$-coated sensors (Figure 3B). However, the predicted data (Figure 3B, "Predicted Data") does not match our observations well ($\alpha > 0.4$). This is apparently due to the assumption of contiguous, homogeneous coatings for all film deposition steps in our model. As the preceding discussion has noted, complete film coverage is not obtained until five PAH/PSS bilayers are adsorbed to the sensor matrix. To account for this, the theoretical predictions for sensitivity were shifted data to the point at which complete coverage is obtained (Figure 3B, "Predicted Data, Shifted"), and the resulting agreement between theoretically predicted and experimentally obtained data is much greater ($\alpha < 0.1$). This further supports the hypothesis that the behavior of {PSS/PAH}$_{0-5}$ sensors arises from incomplete surface coverage; more importantly, this excellent matching also demonstrates the robustness of the theoretical models and the conformity of our system behavior to fundamental phenomena of reaction−diffusion kinetics. Moreover, after homogeneous nanofilm deposition, increasing nanofilm thickness reduces J_G/J_O into the sensor, which increases steady-state local oxygen levels and extends the analytical range.

The data in Figure 3 (both predicted and experimental) suggest a nearly linear relationship between the change in sensitivity and analytical range observed with {PAH/PSS}$_{5-15}$-coated sensors. Linear regression analysis between these data indicated a mean sensitivity change per bilayer of −0.3%/mg dL^{-1} and a mean percent change per bilayer of 11.7 mg/dL. This is indeed remarkable, given the approximate thickness of a single PAH/PSS bilayer is ~2.5 nm when assembled from solutions containing 0.2 M NaCl.[39,41,55] However, this trend was significantly dampened for thicker films, i.e., 15, 20, and 25 nanofilm bilayers, such that the mean changes in sensitivity and analytical range per bilayer were determined to be only −0.03%/mg dL^{-1} and 4.7 mg/dL, respectively. This result can be explained by the incremental reduction of J_G/J_O observed with {PAH/PSS}$_{5-15}$ coatings, where the sequential adsorption of five bilayer increments linearly retards J_G/J_O into the catalytic region of the sensor.[33] However, with nanofilm coatings comprising greater than 15 PAH/PSS bilayers, J_G/J_O begins to be less affected, resulting in a dampened response as predicted in previous work as well as the predicted data presented in Figure 3B.[8] Given this analysis, it is hypothesized that a further increase in the number of nanofilm bilayers would continue to reduce the sensitivity and increase the analytical range, albeit at a less effective rate, a hypothesis supported by our simulation results as well. Specifically, simulation results indicate that 80% of sensitivity tuning is obtained with 5−25 adsorbed nanofilm bilayers, while the adsorption of an additional 75 bilayers (100 bilayers in total) would decrease sensitivity by an additional 10%, indicating that sensitivity modulation through PAH/PSS nanofilm adsorption becomes rapidly inefficient with PAH/PSS bilayers totaling more than 25, a result of the exponential dependence of sensitivity on nanofilm thickness (Figure 3B).

Overall, these results show that nanofilm coating are not required to obtain a glucose-sensitive response, but they are indeed useful in providing a straightforward means to regulate device sensitivity and analytical range as needed. For example, sensors may be rapidly prototyped to cover the hypo- (0−80 mg/dL), normo- (80−120 mg/dL), and hyperglycemic levels (>120 mg/dL) from a single batch of particles by applying different coatings using a few extra adsorption cycles. Therefore, the utility of polyelectrolyte nanofilms in this application cannot be understated. Additionally, it should be noted that alternative applications may employ nanofilms of different composition or adsorption conditions; indeed, a variety of nanocomposite films could be applied to this platform, such that denser or more hydrophobic films could be employed to obtain a similar response with fewer nanofilm bilayers.

Effect of Assembly Solution Ionic Strength and Capping Polyelectrolyte on Sensor Response. In the previous section, variations in nanofilm thickness through sequential adsorption of PAH/PSS nanofilms to the sensor matrix were used to modulate sensitivity and range of microscale enzymatic sensors. Theoretical data indicated that the addition of subsequent nanofilm bilayers greater than 25 would have minimal effect on sensitivity tuning. However, previous work has also shown that changing the ionic strength of assembly conditions as well as varying the capping polymer (terminal layer) could also drastically affect molecular

(53) McAloney, R. A.; Sinyor, M.; Dudnik, V.; Goh, M. C. *Langmuir* **2001**, *17*, 6655−6663.
(54) Arys, X.; Laschewsky, A.; Jonas, A. M. *Macromolecules* **2001**, *34*, 3318−3330.
(55) Loesche, M.; Schmitt, J.; Decher, G.; Bouwman, W. G.; Kjaer, K. *Macromolecules* **1998**, *31*, 8893−8906.

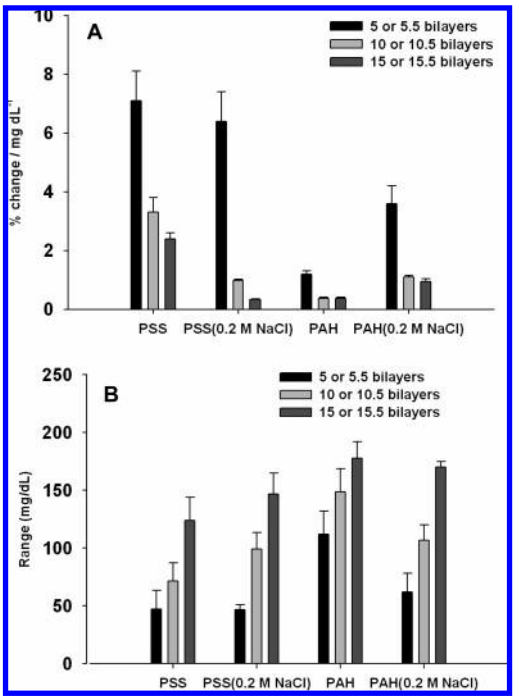

Figure 5. Sensor response characteristics for sensor configurations (A, sensitivity; B, range) based on different capping polyelectrolytes (PAH or PSS), assembly ionic strength (0 or 0.2 M NaCl), and number of nanofilm bilayers (5/5.5, 10/10.5, or 15/15.5) adsorbed to the sensor surface. Note that PSS-terminated films had an integer number of bilayers, whereas PAH-capped films had half-bilayer final values.

transport,[33,39] an observation we hypothesized would afford additional levels of response tunability to these sensing systems.

To investigate the ability to modulate sensor response metrics with assembly using solutions containing salt, and by varying the capping polyelectrolyte, multilayer nanofilms of 5, 10, and 15 bilayers were assembled from solutions of 0 M NaCl or 0.2 M NaCl (as in the previous section) with the capping polyelectrolyte being PAH (as in the previous section) or PSS. Following dynamic testing of each sensor configuration, steady-state glucose response profiles were obtained as before. The sensitivity and analytical range were extracted as before, and the values for each film composition plotted for comparison (Figure 5).

First, it is obvious that the general trend of decreasing sensitivity and increasing range with increasing film thickness is present for all architectures. The changes in sensitivity are significant ($\alpha < 0.05$) for all cases except for PAH-terminated 10.5 and 15.5 films constructed with ($P = 0.065$) and without added salt (identical values, $P = 1$). Increases in range with increasing film thickness are significant ($\alpha < 0.05$) in all cases of coatings constructed with salt, whereas significant differences are only present when comparing the thinnest (5/5.5) and thickest (15/15.5 bilayers) constructed without added salt. Second, when comparing films constructed without added salt, there is also a significant difference between the response properties when films are terminated with PSS and PAH. Specifically, sensors coated with PAH-capped nanofilms are significantly less sensitive ($\alpha < 0.001$) and have significantly wider range ($\alpha < 0.02$) than the counterpart films with PSS final layers, regardless of the number of layers deposited; in these cases, the difference increases with thickness. Since these comparisons are for films varying only by one added layer of PAH, these results suggest that PAH presents a substantial reduction in J_G/J_O, likely due to a different glucose solubility that decreases the partitioning of glucose into the nanofilm coating. This observation matches previous reports, which have noted that the capping nanofilm layer can drastically affect molecular permeabilities; specifically, it was shown that glucose flux through nanofilms terminated with PAH is ~20% less than those terminated with PSS, with a minimal corresponding effect on oxygen transport.[33] Adding one additional layer of PAH to five bilayers results in a film thickness increase of only 10%; however, this small modification leads to a substantial decrease in sensitivity (83%) and an even greater relative increase of the analytical range (138%). Similarly, for 10 and 15 bilayers, the addition of 1 PAH layer results in decreases of 88 and 84% in sensitivity and increases in the range of 108 and 44%, respectively. It can be noted that the percentage increase in range is smaller for a higher number of bilayers, which is generally expected as the diffusion barrier increases for increased number of layers.

In contrast, when salt is added to the assembly solutions, two important trends are evident. First, when comparing films assembled without salt to identical architectures constructed with added salt, the sensitivity decreases and increases for PSS and PAH, respectively, while the range values are inversely related. These differences in sensitivity are significant ($\alpha < 0.005$) for all cases except five-bilayer PSS-terminated films ($P = 0.44$); for range, the differences are significant ($\alpha < 0.05$) except for the thickest films (15 and 15.5 bilayers, $P > 0.2$) and the five-bilayer PSS-terminated films ($P = 0.96$). Second, the differences are much less pronounced when comparing films with different terminal materials that were deposited from salt-containing solutions than those deposited without salt; in fact, no significant difference ($\alpha < 0.05$) was obtained in any case.

These observations suggest some interesting influences of the nanofilms on glucose transport. First, it is noteworthy that films assembled with 0.2 M NaCl have been reported to possess a 25% increased thickness—from 2 to 2.5 nm for each bilayer—than those assembled in the absence of NaCl;[39,41,55] therefore, if the changes were purely related to film thickness (i.e., not changes in film density), the relative flux would be expected to decrease with added salt. This explanation could arguably match the observations for PSS-terminated films, excluding the five-bilayer case. This latter case could be a special situation where the five-bilayer films without salt did not yet arrive at homogeneous coverage, resulting in a similar effect (decreased oxygen delivery relative to glucose) and response, as described in the previous section. The expected trend of decreased sensitivity due to relative increase in film thickness is observed when 10 and 15 PSS-capped nanofilm bilayers assembled without salt and with 0.2 M NaCl are adsorbed to the sensor surface.

On the contrary, when comparing response characteristics of films capped with PAH layers, the opposite trend is observed: a significant increase in sensitivity is seen when salt is added. A change in thickness with added salt cannot explain this behavior; a decrease in film density with salt would match these results, but this explanation would fall short for PSS-terminated films. Thus, neither of these phenomena can explain the observations in every case.

A final comparison suggests a third possible reason for the observed behavior. When comparing films constructed from solutions with added salt, the differences between films terminated with different materials are much less substantial than in the no-salt case. The range values are not significantly different when comparing films of the same number of coating cycles, and the sensitivity values vary little. In fact, if we consider the no-salt cases to represent films with a "purer" outer surface of the terminal material, the trend that is observed when salt is added is the films look more like the other material present in the film. In other words, the addition of salt appears to blend the contributions of the materials present, effectively averaging the individual effects and thereby reducing the significance of the capping layer in determining the overall glucose flux. This concept is supported by other reports on the increasing interdigitation of nanofilm layers with thickness and adsorption solution ionic strength.[41,55,56] In brief, added counterions screen charges along the polyelectrolyte chains, resulting in increasing coiling and folding of molecules. Films assembled using more coiled molecules have more looping and protruding regions, and are less dense, which means they are thicker, lower density have less internal compensation (pairing of ionized moieties with those from previously adsorbed molecules) and allow more penetration from adsorbing molecules. Thus, the materials have less discrete boundaries (this is why they have been called "fuzzy"), and therefore, the contributions of the individual layers are less discrete as well. While additional work on direct measurements of glucose flux and diffusion coefficients through various film architectures is currently in progress, these findings suggest several different means of tuning nanofilm transport properties to precisely engineer sensor response characteristics: thickness, adsorption conditions, composition, and terminal layer.

Effect of Bulk Oxygen Levels on Glucose Response. It is well-known that local oxygen supply within the dermis is highly dependent on atmospheric conditions as well as depth, with concentrations fluctuating from 215 (near the epidermis−dermis junction) to 90 μM (near vasculature).[57] Since the reported system relies on oxygen measurements to indirectly determine glucose levels, it is important to examine sensor performance during exposure to varying bulk oxygen concentrations. Following stabilization of bulk oxygen levels below (90 μM), at (257 μM), and above (540 μM) atmospheric concentration, sensors were exposed to random step changes in bulk glucose levels and the sensitivity and range calculated (Figure 6A). Furthermore, simulation results obtained by varying bulk oxygen levels were normalized and plotted with normalized experimental results for comparison (Figure 6B).

As expected, these data, both predicted and experimental, suggest that glucose response significantly varies with changes in bulk oxygen levels, an observation noted in similar enzymatic-based sensing systems.[58,59] Again, we observe high correlation ($\alpha < 0.02$) between predicted and experimental data (Figure 6B), indicating the ability of the diffusion−reaction model to predict

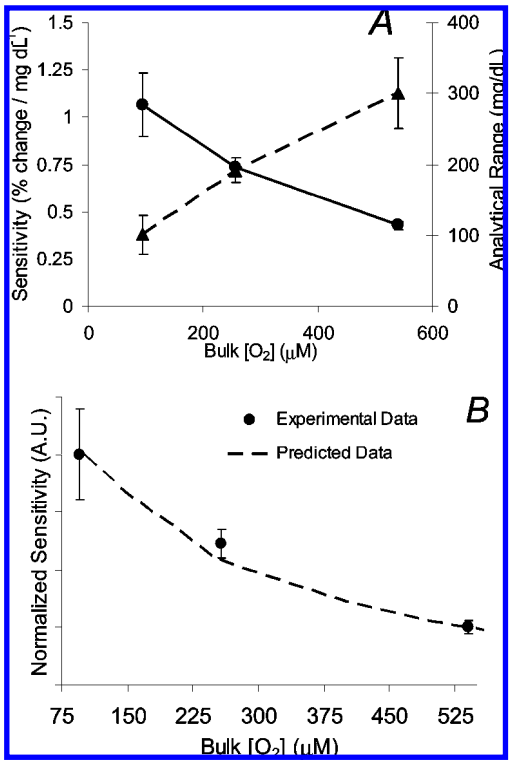

Figure 6. (A) Effect of bulk oxygen levels on sensitivity (●) and analytical range (▲), acquired from sensors with 25 PAH/PSS nanofilm bilayers. Error bars donate one standard deviation of triplicate measurements. (B) Comparison of normalized predicted (▲) and experimentally obtained (●) sensitivity profiles of sensors coated with 25 PAH/PSS nanofilm bilayers.

the effect of varying physical parameters on device performance. In the experimental data, a 60% decrease in sensitivity at a rate of 0.14%/mg dL^{-1} per 10 μM oxygen and 200% increase in analytical range at a rate of 44.1 mg/dL per 10 μM oxygen were observed when evaluating sensor performance over the tested range of bulk oxygen levels. This occurrence can be simply explained by variations in local oxygen levels induced by changes in the bulk. At elevated bulk oxygen levels, the average steady-state oxygen concentration within the sensors is elevated;[8] therefore, higher incremental glucose levels are required to significantly reduce the elevated average oxygen level within the sensor, increasing the analytical range and subsequently decreasing sensitivity.

A more physiologically relevant demonstration is the comparison of response properties acquired at 95 and 257 μM bulk oxygen levels, respectively, which constitute a 31% decrease in sensitivity and a 90% increase in analytical range. Using the predicted response data within this physiologically significant range (Figure 6B), it is evident that the sensors operate with a linear dependence ($\alpha < 0.02$) on bulk oxygen levels, indicating that the sensing scheme is not reaction-limited (i.e., GOx is unsaturated) but is rather diffusion-limited, as desired. Further simulation data suggest the onset of reaction-limited kinetics at bulk oxygen levels greater than 500 μM, an oxygen level far greater that physiological levels. This excess enzymatic capacity is a useful design feature for increasing the longevity of enzymatic-based systems, such that subsequent loss of enzymatic activity resulting from GOx inactiva-

(56) Gopinadhan, M.; Ivanova, O.; Ahrens, H.; Guenther, J.-U.; Steitz, R.; Helm, C. A. *J. Phys. Chem. B* **2007**, *111*, 8426−8434.
(57) Stucker, M.; Struk, A.; Altmeyer, P.; Herde, M.; Baumgartl, H.; Lubbers, D. W. *J. Physiol. (London)* **2002**, *538*, 985−994.
(58) Li, L.; Walt, D. R. *Anal. Chem.* **1995**, *67*, 3746−3752.
(59) Healey, B. G.; Li, L.; Walt, D. R. *Biosens. Bioelectron.* **1997**, *12*, 521.

tion would not immediately affect sensitivity.[8,46,60−63] Furthermore, these data suggest that natural bulk oxygen variations in skin would make stable in vivo calibrations difficult to obtain. Thus, these findings, although expected, indicate the importance of having an internal oxygen reference to compensate for response artifacts due to natural fluctuations in in vivo bulk oxygen levels.

While the development of internally oxygen referenced sensors is ideal to compensate for bulk oxygen fluctuations, in practice, this may prove difficult using steady-state fluorometry, as spectral deconvolution between glucose sensing and oxygen compensation data is not straightforward. A possible short-term solution is to minimize the effect of bulk oxygen levels on sensor response by decreasing sensitivity dependence on bulk oxygen concentrations. The data in Figure 6B suggest a 12% decrease in sensitivity per 10 μM bulk oxygen ($\alpha < 0.02$); should this dependence be reduced (or eliminated), the attractiveness of these devices for in vivo monitoring would be significantly enhanced. To achieve this ideal, further reduction of J_G/J_O would be desired, resulting in lower sensitivities and greater ranges (i.e., reduced onset of oxygen-limited consumption) and subsequently reduced dependence of response metrics on bulk oxygen levels. However, the results reported in this work indicate that further reduction of J_G/J_O with additional PAH/PSS nanofilms would be inefficient (due to exponential dependence of sensitivity on nanofilm bilayers, Figure 3B). A unique approach, which would have the same effect as reducing J_G/J_O, would involve incorporating catalase (Cat), an enzyme that consumes hydrogen peroxide and produces water and oxygen, to form third-generation bienzymatic smart tattoos. A bienzymatic GOx- and Cat-based sensing scheme would reduce the net consumption of oxygen by half (Scheme 1), resulting in higher relative local steady-state oxygen levels for given bulk glucose levels and subsequently reducing the onset of oxygen-limited consumption and extending analytical range, a result similar to reducing J_G/J_O into the catalytic region of the sensor. Furthermore, it is well-known that enzymatic-based systems, such as those reported in this work, are susceptible to spontaneous inactivation and inactivation due to pH and hydrogen peroxide, resulting in response instability over time.[46,60−63] In the case of GOx, however, previous work indicates that hydrogen peroxide,

Scheme 1. Comparison of Glucose Consumption Kinetics within Sensors Containing Immobilized GOx (Top) and Coimmobilized GOx and Cat (Bottom)[a]

$$\text{Glucose} + O_2 + H_2O \xrightarrow{\text{GOx}} \text{Gluconic Acid} + H_2O_2$$

$$\text{Glucose} + \frac{1}{2}O_2 \xrightarrow{\text{GOx and Cat}} \text{Gluconic Acid}$$

[a] Note the overall reduction in molecular oxygen consumption with the bienzymatic (GOx and Cat) scheme.

a compound broken down by Cat, is the more aggressive inactivant.[46,60−63] Thus, we hypothesize an optimized a bienzymatic sensing scheme composed of GOx and Cat could further extend sensor analytical range (by reducing net oxygen consumption) and enhance response longevity (by consuming hydrogen peroxide) when compared to those of this work, enhancing the clinical attractiveness of this technology. The results of this ongoing study will be reported in an additional installment.

CONCLUSION

Highly sensitive microparticle enzymatic sensors with tunable response properties have been demonstrated using glucose as a model analyte. These sensors rely on optical transduction of oxygen levels within microscale sensors to indirectly determine bulk glucose levels. To obtain glucose-limited oxygen within the sensors, mass transport-limiting nanofilms were adsorbed to the sensor surface. By simply adjusting film assembly conditions, device sensitivity could be tuned to pinpoint hypo- (0−80 mg/dL), normo- (80−120 mg/dL), and hyperglycemic levels (>120 mg/dL), with good agreement with theoretical predictions. Given the scalability of this platform, similar devices targeting other biochemicals can be obtained by selecting respective oxidases and the response properties tuned using a straightforward and cost-effective means—polyelectrolyte nanofilms. Furthermore, this technique is not limited to the confines of microscale optical sensing technology, but is broadly applicable to other technologies that would benefit from the precise control of substrate transport, such as electrochemical sensing and filtration processes.

ACKNOWLEDGMENT

The authors acknowledge the NIH (R01 EB000739) for financial support

Received for review August 17, 2007. Accepted December 14, 2007.

AC701738E

(60) Gouda, M. D.; Singh, S. A.; Rao, A. G.; Thakur, M. S.; Karanth, N. G. *J. Biol. Chem.* **2003**, *278*, 24324−24333.
(61) Tse, P. H. S.; Leypoldt, J. K.; Gough, D. A. *Biotechnol. Bioeng.* **1987**, *29*, 696−704.
(62) Kleppe, K. *Biochemistry* **1966**, *5*, 139−143.
(63) Miron, J.; Gonzalez, M. P.; Vazquez, J. A.; Pastrana, L.; Murado, M. A. *Enzyme Microb. Technol.* **2004**, *34*, 513−522.